2-Deoxyribose-5-phosphate aldolase from *Thermotoga maritima* in the synthesis of a statin-side chain precursor: characterization, modelling and optimization

Short title: DERA^{Tm} in the synthesis of a statin-side chain precursor

Anera Švarc[1], Zvjezdana Findrik Blažević[1], Đurđa Vasić-Rački[1], Anna Szekrenyi[2], Wolf-Dieter Fessner[2], Simon J. Charnock[3], Ana Vrsalović Presečki[1*]

[1]University of Zagreb, Faculty of Chemical Engineering and Technology, Savska c. 16, HR-10000 Zagreb, Croatia

[2]Technische Universitaet Darmstadt, Institute for Organic Chemistry and Biochemistry, Alarich-Weiss Str 4, D-64287 Darmstadt, Germany

[3]Prozomix Ltd, Stn Court, Haltwhistle NE49 9HN, Northumberland, England

[*]**Corresponding author:**
Ana Vrsalović Presečki
Faculty of Chemical Engineering and Technology, University of Zagreb
Savska cesta 16, HR-10000 Zagreb, Croatia
tel.: 00385 1 4597 157
e-mail: avrsalov@fkit.hr

Abstract

BACKGROUND: The statin side-chain synthesis by the sequential aldol condensation catalyzed by DERA (EC 4.1.2.4) is the most known and promising route. The advantage of this process is the formation of two stereocenters in a single step starting from inexpensive achiral components, acetaldehyde and chloroacetaldehyde. The limitation for the industrial-scale application is enzyme inactivation caused by substrates as well by the intermediate produced by single aldol addition.

This article has been accepted for publication and undergone full peer review but has not been through the copyediting, typesetting, pagination and proofreading process, which may lead to differences between this version and the Version of Record. Please cite this article as doi: 10.1002/jctb.5956

RESULTS: DERA enzyme from *Thermotoga maritima* (DERA^{Tm}) was extensively investigated in this work. The influence of aldehydes on DERA^{Tm} stability was studied in detail. Based on experimentally determined kinetic parameters of all reactions included in the synthesis of statin side chain, mathematical models in different reactor configurations were developed. Models also include enzyme inactivation by all compounds that have negative impact on its stability. Mathematical model-based optimization enabled finding the optimal process conditions and choosing the best reactor configuration. The fed-batch reactor proved to be the most suitable choice. Under optimal conditions product concentration of 78 g/L, productivity of 56 g/(L day) and yield of 95% was achieved.

CONCLUSION: The validated mathematical model and the used methodology can be exploited for further process improvement and for process design of similar systems.

Key words: biocatalysis, kinetics, mathematical modelling, process intensification, enzymes, optimization

1. Introduction

The aldol reaction has long been recognized as one of the most powerful methods of forming useful carbon-carbon bonds. [1-10] Aldolases, a group of naturally occurring enzymes that catalyze *in vivo* aldol reactions, [1,7,10] are capable of exhibiting high regio- and stereoselectivity under mild conditions with minimal use of protecting group chemistry, and therefore are an interesting alternative to chemical aldol synthesis. [3-5,9-11] 2-Deoxyribose-5-phosphate aldolase (DERA, EC 4.1.2.4) is the only known member of the aldolase family using acetaldehyde as a nucleophile [1,2,8-10,12] and the only aldolase known to accept three aldehydes in a sequential and stereo-selective manner for a cascade aldol reaction [1-5,7,12-15] without the use of any cofactors. [10,16] Interestingly, DERA catalyzes reactions in which both substrates and resulting products are aldehydes, [1,4,7,8,10,11,17] which is unusual among aldolases, [7,8,10] with the exception of engineered D-fructose-6-phosphate aldolase variants. [7] DERA accepts a broad range of acceptor

aldehydes, [1,5,7, 9-11,16,18-20] has a relatively large donor tolerance [1,8,10,11,17,20] for compounds having up to four carbon atoms, and generates (*R*)-configured chiral centers. [7, 8, 19] Therefore, it is not surprising that much attention has recently been given to its application for the synthesis of valuable chiral molecules. [1,5,11,12,14-19]

By using achiral substrates, like chloroacetaldehyde and acetaldehyde, [4, 21] DERA catalyzes a sequential aldol addition that results in an enantiomerically pure lactol, (3*R*,5*R*)-6-chloro-2,4,6-trideoxyhexose. [7,16,18,22,23] This 2,4,6-trideoxyhexose is a valuable chiral synthon for HMG-CoA reductase inhibitors, [5,6,18] collectively known as statins, [6] and used for the production of cholesterol-lowering drugs, such as atorvastatin and rosuvastatin. [5-7,10,13-16,19,22] Those statins have an approximately US$20 billion worldwide sales, [6, 13] among which the Pfizer's Lipitor (atorvastatin calcium) was the world's top-selling drug [6,13,22] with revenues over US$10 billion per year. [13,22] Therefore, the preparation of the 2,4,6-trideoxyhexose has attracted an immense effort because of its extremely high market price and the requirement for high chemical and stereochemical purity at its two chiral centers. [3,6,21] Since the chemical synthesis of statins is time-consuming and consists of a number of synthetic steps that are carried out at very harsh conditions, [3,4,20,24,25] the use of DERA for the synthesis of the statin side chains presents one of the most attractive and promising routes, [1,3,5,6,9,13,19-21] due to its ability to introduce both stereocenters in a single step. [1,3,5,6,9,19-21]

Although DERA-catalyzed reactions offer an attractive alternative to chemical methods for the synthesis of chiral statin side-chain precursors, [1,5,6,12,14,19,22] practical applications of DERA are still limited. [14, 21] DERA shows poor resistance to high aldehyde concentrations [3,6,12,14,15,20] and low catalytic efficiency toward the sequential aldol addition of unnatural substrates. [6,21,23] Thus, large quantities of the enzyme are necessary to obtain industrially useful product yields. [3,6,14,17,20,21,23] This issue can be circumvented by improving its resistance and catalytic activity using a molecular evolution approach [3,23,26], or by applying a

cell-free lysate or a whole cell biocatalyst instead of an isolated enzyme [4,20] or by immobilization on appropriate supports. [27-30]

In pursuit of finding the most cost-effective configuration for the lactol synthesis, especially for industrial use, it is of great importance to understand the mechanisms and kinetics of enzyme systems in detail, which can be achieved by applying mathematical modelling techniques. [31-33] Although the lack of reports on kinetic data obtained from kinetic models of DERA-catalyzed reactions is evident, [3] some kinetic studies of related aldolase-based syntheses can be found. [3,34,35] Ručigaj and coworkers (2015) have reported a very complex model for the sequential aldol reaction involving acetyloxyacetaldehyde, acetaldehyde and chloroacetaldehyde as substrates, which was catalyzed by crude DERA expressing culture lysate. [3]

The aim of this work was to optimize the production of the statin precursor (**4**) from acetaldehyde (**1**) and chloroacetaldehyde (**2**) in the reaction catalyzed by the DERA from *Thermotoga maritima* (DERA^{Tm}) (Figure 1), a hyperthermophilic organism that shows great potential to serve as a new source of highly stable enzymes. [15] For this purpose it was necessary to characterize the enzyme, investigate the effect of reaction conditions and to develop a mathematical model of the DERA-catalyzed synthesis of a statin side-chains precursor, which can be further used as a useful tool in designing a suitable process system for the investigated reaction.

Figure 1.

2. Materials and methods

2.1 Chemicals

3-Deoxyribose-5-phosphate, acetaldehyde, chloroacetaldehyde, KH_2PO_4 were purchased from Sigma-Aldrich (Germany), tris(hydroxymethyl)aminomethane, NADH, triethanolamine hydrochloride, trifluoroacetic acid, pyridine, *o*-benzylhydroxylamine hydrochloride from Acros Organics (USA), K_2HPO_4 from Merck (Germany), acetonitrile from VWR Chemicals (France), methanol from J.T.Baker (Poland), triosephosphate isomerase from rabbit muscle and α-glycerol-3-phosphate dehydrogenase from rabbit muscle from Sigma-Aldrich (Germany), while DERA^{Tm} was provided by Prozomix.

2.2 HPLC measurements

Samples (5 µL) taken at regular time intervals were mixed with 50 µL of a stock solution of *o*-benzylhydroxylamine hydrochloride (0.02 g/mL in a mixture of pyridine/methanol/water 33/15/2) for derivatization. [36] After incubation on a shaker at 25 °C for 20 min, samples were diluted with methanol (450 µL), centrifuged and analyzed by HPLC (Phenomenex LiChrospher C18 column, 5 µm, 250 x 4 mm). The mobile phase consisted of solvent A (0.1% v/v trifluoroacetic acid (TFA) in acetonitrile) and solvent B (0.1% v/v TFA in water) with gradient elution from 90 to 28.4 %B for the first 22 minutes and from 28.4 to 90 %B from minute 22 to 25. The flow rate was 1.2 mL/min, the column temperature was set at 30 °C, and the UV detection at 215 nm.

2.3 Enzyme assay and determination of protein concentration

The DERA^{Tm} activity was determined by using the 3-deoxyribose-5-phosphate (DRP) assay [15] (assay 1) or in the reaction of aldol addition of **1** to **2** (assay 2).

Assay 1: The DRP cleavage activity of DERA^{Tm} was determined at 25 °C by measuring the oxidation of NADH in a coupled assay using triose-phosphate isomerase (TPI) and glycerol-3-phosphate dehydrogenase (GDH), as described in the literature. [14-16] The assay mixture contained 0.1 M TEA-HCl buffer, pH 7, 0.1 M NADH, 0.4 mM DRP, 11 U of TPI, 4 U of GDH, and diluted DERA^{Tm}. The reaction was

initiated by the addition of DERA^{Tm}, and the subsequent decrease of NADH concentration was monitored at 340 nm. 1 U of DERA^{Tm} activity was defined as the amount of enzyme required for cleavage of 1 µmol of DRP per minute in 0.1 M TEA-HCl buffer pH 7 and at 25 °C.

Assay 2: The DERA^{Tm} activity in the aldol addition reaction was determined by monitoring a synthetic reaction with 200 mM of **1** and 100 mM of **2** in the indicated buffer at 25 °C. The reaction was initiated by enzyme addition (1 mg/mL). Samples were withdrawn at regular time intervals during the first 10 mins of the reaction and analyzed by HPLC. 1 U of DERA^{Tm} activity was defined as the amount of enzyme required to form 1 µmol of product per minute at 25 °C and in the selected buffer.

Protein concentration was determined according to the Bradford's assay. [37]

2.4 Influence of pH and temperature on DERA^{Tm} activity and stability

The effect of different buffers and pH on DERA^{Tm} activity and stability was investigated in 0.1 M TEA-HCl buffer (pH 7), 0.1 M phosphate buffer (pH 5.4, 6, 7, 8) and 0.1 M Tris-HCl buffer (pH 7, 8, 9). The effect of temperature on DERA^{Tm} activity and stability was examined in the interval between 20 and 50 °C, with steps of 5 °C.

The DERA^{Tm} activity in buffers of different pH was determined according to assay 2 by following the rate of product formation. DERA^{Tm} stability was determined by using assay 1 in the following manner. DERA^{Tm} (10 mg/mL) was dissolved in buffer and incubated at 25 °C, and the residual activity was determined after 24 hours.

To assess the enzyme thermostability at different temperatures, enzyme preparations in 0.1 M TEA-HCl buffer (10 mg/mL, pH 7) were incubated for 6 days during which the residual activity was determined at appropriate intervals using assay 1. To evaluate the activity at different temperatures, DERA^{Tm} (10

mg/mL) was incubated for 5 min at different temperatures after which residual activity was determined at 25 °C by using assay 1.

2.5 Influence of aldehydes on DERA^{Tm} stability

The effects of **1**, **2**, 4-chloro-3-hydroxybutanal (**3**) and 6-chloro-3,5-dihydroxyhexanal (**4**) on the stability of DERA^{Tm} were examined. Enzyme preparations in 0.1 M TEA-HCl buffer (10 mg/mL, pH 7) containing different amounts (0 – 800 mM) of each single aldehyde (**1**, **2**, **3** or **4**) were incubated at 25 °C for 3 hours. Samples were taken at regular time intervals and activity measured using assay 1 in order to determine the enzyme operational stability decay constant. Before the activity measurements aldehydes were removed by using the Amicon Ultra-0.5 Centrifugal Filter Units (MWCO 10 kDa), and the enzyme residue was diluted in buffer to be used for the assay.

2.6 Kinetic analysis

Kinetic parameters were estimated from the initial reaction rates vs concentration data in the aldol additions of **1** to **2** (the first addition of **1**) and of **1 to 3** (the second addition of **1**), as well as in the self-aldol addition of **1** catalyzed by crude DERA^{Tm} occurring as a side reaction. The initial rates were calculated from the change of product concentration in the first reaction period when the substrate conversion was less than 10% (assay 2). Product concentrations were determined by HPLC analysis. The obtained initial rates were fitted to the Michaelis-Menten kinetic models. One unit of DERA^{Tm} activity was defined as the amount of enzyme necessary to produce 1 µmol of product per minute in 0.1 M TEA-HCl buffer and at 25 °C.

2.7 Reactor experiments

The aldol reaction was carried out in three different reactor configurations: batch, repetitive batch and fed-batch. The reactions were performed at 25 °C using crude DERA^{Tm} in 0.1 M TEA-HCl buffer at pH 7. In

batch reactor (1 mL; 1.5 mL microcentrifugal tube) the reaction mixtures contained 200 mM **1** and 100 mM **2** with 1, 2, 5, 10, 15 or 20 mg/mL of DERA^{Tm}. In case of repetitive batch reactor (3 mL; 15 mL conical centrifugal tubes), the reaction was carried out with three portions of substrate (200 mM **1** and 100 mM **2**) and enzyme (5 mg/mL) additions. In the fed-batch reactor (50 mL glass bottle), the initial reactor volume was 6 mL containing only buffer. The substrates (feed 1: 5 µL/min; 2450 mM **1**, 950 mM **2**) and the enzyme (feed 2: 2 µL/min; 100 mg/mL) were pumped separately into the reactor using two piston pumps (PHD 4400 Syringe Pump Series, Harvard Apparatus). The experiment was monitored for 33 h and the final reaction volume was 20 mL.

In all reactor experiments samples were withdrawn at regular time intervals and analyzed by HPLC. The residual enzyme activity was determined at appropriate intervals using the DRP assay.

2.8 LC-MS analysis

The analysis of the derivatized products was done using the LC-MS analysis (Phenomenex Kinetex Core-shell C18 column, 2.6 µm, 100 x 4.6 mm). HPLC with diode array detector (DAD) and MS detection (Shimadzu LCMS-2020 single quadrupole liquid chromatograph mass spectrometer) was used. The selected ion monitoring method was used to confirm molecular weight of the derivatized peaks of formed products. The mobile phase consisted of solvent A (0.1% v/v formic acid in water) and solvent B (0.1% v/v formic acid in acetonitrile) with gradient elution from 90 to 19 %A for the first 10 minutes and from 19 to 90 %A from minute 14 to 16. The flow rate was 0.5 mL/min, the column temperature was set at 30 °C, and the UV detection at 215 nm. The mass spectrophotometer was equipped with electrospray ionization (ESI) source and operated in positive polarity mode. ESI conditions were: capillary voltage 4 kV, nebulizing gas flow 1.5 L/min, drying gas flow 15 L/min, temperature 300 °C.

2.9 Data processing

The kinetic parameters of the Michaelis-Menten kinetic models (V_m, K_m, K_i) were estimated from the independent initial reaction rate data by nonlinear regression analysis using the simplex or least squares method implemented in MicroMath *Scientist* software.[38] Parameters V_m and K_m were estimated from the dependence of the initial reaction rate on substrate concentration using the Michaelis-Menten kinetics whereby no inhibition occurred. In the case of two-substrate Michaelis-Menten kinetics, V_m and two K_m's were estimated from two sets of measurements in which one substrate concentration was kept constant, while the other was varied. The inhibition constant was estimated from the dependence of the inhibitor concentration on the initial reaction rate. Each individual constant was evaluated from one set of measurements using the Michaelis-Menten equation with the included effect of only one inhibitor. During the estimation of the K_i constant, V_m and K_m values were used as fixed values estimated from independent measurements as described above.

The operational stability decay constants (k_d) were estimated by using the experimental data of activity *vs* time.

The set of optimum parameters were used for the simulation according to the proposed models. For simulations the built-in *Episode* algorithm for stiff system of differential equations was used. Standard deviations (σ) and coefficients of determination (R^2) as measures of goodness-of-fit were calculated by *Scientist* built-in statistical functions.

3. Results and discussion

In this work the consecutive aldol reaction system catalyzed by DERA^{Tm} was studied, in which the acceptor substrate **2** reacts in a first step with the donor substrate **1** to give the adduct **3**, [6,9,14,19] which subsequently reacts with a second equivalent of the donor **1** to result in the key product **4** (Figure 1). [1] Spontaneous cyclization of **4** after the second addition step of **1** to **3** drives the overall equilibrium favorably because the high stability of the cyclized lactol form of the final product removes the open-

chain **4** from the aldol equilibrium. [1,4,6,8,10,12,14,15,18,19] For the same reason, a further, third addition step of **1** to **4** is prevented. [1,5,8,9,19,39] Due to the nature of the donor substrate, which can also act as an acceptor substrate, the DERA-catalyzed self-aldol addition of **1** occurs as a side reaction (Figure 2). [5,14,15] The reaction of **1** self-addition is a 2-step reaction in which first an intermediate is formed and then consecutively the final product 3,5-dihydroxyhexanal (**5**). When the reaction was conducted with DERA^{Tm}, the formation of the intermediate was in a very small amount and therefore was neglected.

Figure 2.

3.1 Influence of pH and temperature on DERA^{Tm} activity and stability

To find optimal conditions for the DERA^{Tm} catalyzed reaction, the enzyme activity and stability in different buffers (pH 5.4 – 9.0) (Supplement Fig. S1 – S2) and at different temperatures (20 – 50 °C) were investigated (Supplement Fig. S3 – S4). The enzyme DERA^{Tm} showed the highest activity in 0.1 M TEA-HCl buffer at pH 7.0 in the tandem reaction of **2** with **1**, which is in agreement with the previously published codon-optimized DERA. [16] The activity increased with rising temperatures in accordance with the Arrhenius equation (Supplement Fig. S3). The enzyme showed very good thermostability and pH stability. More than 80% of its initial activity was retained after 67 h of incubation at temperatures in the range between 20 and 40 °C, with highest residual activity at 20-25 °C (≈ 87%) (Supplement Fig. S4), rendering the DERA^{Tm} more thermostable than the corresponding DERA from *Lactobacillus brevis*. [21] It was found that the residual enzyme activity was practically constant (>80%) within the pH range from 5.4 to 8.0 and 24 h of incubation, which also is in accordance with previous investigations. [15] The highest residual activity (96%) was noticed in 0.1 M TEA-HCl buffer at pH 7.0 at 25 °C (Supplement Figs. S3 – S4). Because of these facts, and taking into consideration the volatility of **1** (bp = 20.2 °C), further investigations were performed in 0.1 M TEA-HCl buffer, pH 7.0 at 25 °C.

3.2 Experiments in batch reactor with different DERA concentration

It was reported that lower amounts of DERA decrease the amount of product **4** arising from the second aldol reaction. [19,25] Therefore, to find the optimal DERA^{Tm} concentration for obtaining the highest concentration of **4**, and to minimize the enzyme operational stability decay, several reactions were performed in a batch reactor using same initial substrate concentrations but different initial DERA^{Tm} concentrations.

The results (Figure 3) show that enzyme concentrations above 5 mg/mL result in high product concentration, while enzyme operational stability decay is less prominent. These results implicate that DERA stability is significantly affected by the presences of substrates. [2,3,15,20,25] Lower DERA^{Tm} concentration causes a lower consumption rate for **1** and **2** and, as a consequence, the enzyme is longer exposed to the negative influence of the aldehyde substrates. [4,25]

Figure 3.

3.3 Impact of aldehydes on DERA^{Tm} stability

Because of these findings and previous observations reported in the literature [15,20] the individual influence of **1**, **2**, **3** and **4** on the enzyme stability was examined. The purpose of these measurements was to define the operational DERA stability in order to predict the enzyme behavior in the reactor. Within these measurements, the mechanism of inactivation which has not yet been fully clarified,[30] was not investigated. It was found that **1**, **2** and **3** have a negative effect on the enzyme stability, whereas **4** has practically no effect (data not shown). Three models were tested for describing the enzyme inactivation: the first-order decay kinetics, the second-order decay kinetics and the parallel model (three-parameter biexponential equation). [40] The second-order decay kinetics and the parallel model resulted with almost the same goodness-of-fit to the experimental data. Due to less number of parameters, the decrease of DERA^{Tm} activity during incubation with **1**, **2** and **3** was described by second-order kinetics. Due to less number of parameters, the decrease of DERA^{Tm} activity during incubation with

1, **2** and **3** was described by second-order kinetics. The operational stability decay constant k_d was estimated form the experimental results of relative activity (*A*) vs time for each aldehyde concentration. The presented results show the dependence of k_d on the concentration of **1**, **2** and **3**, described by a second-order polynomial model (Figure 4). The estimated parameters of the polynomial model (Eq. 1) are presented in Table 1.

Figure 4.

Table 1.

It was noted that the concentrations of **1** and **2** of up to 100 mM influence the enzyme stability considerably, which is in accordance with previous findings for the DERA enzyme. [25] Substrate **2** was found to be a more potent deactivator of DERA^{Tm} as compared to **1**. This was also the case with previous investigations with DERA enzymes from various sources. [2,3,21,25] The operational stability decay by **1** is consistent with previous research carried out with DERA^{Tm}. [15] More interestingly, the results indicate that **3** has a higher destabilizing effect on DERA^{Tm}, compared to either **1** or **2**. Hence, it is of crucial importance to select optimal initial substrate concentrations and the suitable reactor configuration to avoid accumulation of the intermediate **3** in the reactor.

3.4 DERA^{Tm} kinetics

The kinetic investigation of the DERA^{Tm}-catalyzed aldol addition of **1** to **2** was carried out to develop a mathematical model that will be applicable for different reactor configuration. Since the DERA-catalyzed statin side-chain production is considered to be a very complex reaction system, the formal kinetic model was applied. During the DERA-catalyzed reaction many compounds are being produced and spent resulting in a system with a large number of possible interactions. Applying the mechanistic model for its description would result with number of parameters[3] wherefore it is hard to get intrinsic control of

correctness in its estimation. The formal kinetic model includes the data-driven or the empirical model which has less kinetic constant. [41] Those constants can be independently evaluated and have a defined physical meaning. So, in order to describe the kinetics in the explored process, one- or two-substrate Michaelis-Menten equations were used.

The experiments were carried out in a batch reactor by adding different amounts of reactants **1**, **2** and **3**. By using the initial reaction rate method, the influence of different concentrations of **1** and **2** or **1** and **3** on the specific DERA^{Tm} activity of the first (Figure 5 A) and second (Figure 5 B) addition, respectively, were determined. Since DERA^{Tm} can also utilize **1** as an electrophilic aldol component (Fig. 2), and thus can catalyze a direct self-aldol addition to produce 3,5-dihydroxyhexanal (**5**) over two steps, the kinetics of this side reaction (Fig. 6) was examined as well.

Figure 5.

The kinetics of the first (Fig. 5 A) and second step (Fig. 5 B) of DERA^{Tm}-catalyzed aldol reaction were described by two-substrate Michaelis-Menten kinetics (Table 2, Eqs. 2 and 3), while the kinetics of the DERA^{Tm}-catalyzed reaction of self-addition of **1** (Figure 6) was described by one-substrate Michaelis-Menten kinetics with competitive inhibition of **2** and non-competitve inhibition of **3** (Table 2, Eq. 4). The types of inhibition were determined from the Lineweaver–Burk plots (supplement, Fig. S5). The values of estimated kinetic parameters are given in Table 2. The DERA^{Tm}-catalyzed retro-aldol reaction does not occur (data not shown). Product **4** does not inhibit the first or the second aldol addition.

Figure 6.

Table 2.

The maximal rate of DERA^{Tm} in the first addition of **1** in the reaction with **2** was 5.5-fold higher than the maximal rate of the second addition step (Table 2). Because of that, accumulation of **3** is to be expected.

[20] The maximum rate of self-aldol addition of **1** was somewhat higher than the rates of the aldol additions of **2** with **1** (V_{m1} and V_{m2}) but due to severe inhibition by **2** (K_{i3}^{2}) this reaction will not be the preferred one. [16] This suggests that the preferred reaction is the addition of **1** to **2**.

3.5 Validation of the developed mathematical model

The kinetic model of the tandem aldol addition catalyzed by DERA^{Tm} includes: (i) kinetics of formation for **3** (Eq. 2), (ii) kinetics of formation for **4** (Eq. 3) and (iii) kinetics of formation for **5** (Eq. 4). [3] To complete mathematical models of the aldol reaction of **2** with **1** mass balance equations for batch and fed-batch reactor configurations were set based on reaction schemes (Figs. 1-2, Table 3). The operational stability decay of DERA^{Tm} was described by second-order kinetics (Eqs. 10 and 16). The dependency of the operational stability decay rate constant on the concentration of **1**, **2** and **3** was also included in the model (Eq. 18).

The mathematical models (Tables 2 and 3) were validated in a batch, repetitive batch (Eqs. 2-10 and Eq. 18) and fed-batch reactor configuration (Eqs. 2-4 and Eqs, 11-18).

Table 3.

The model validation in the batch reactor is shown in Figure 7. Complete conversion of **1** and **2** was achieved after 1.2 hours. The intermediate **3** was not completely transformed into **4** due to a lack of **1**, which was also consumed in the side reaction (Fig. 2). The yield on the desired product **4** with respect to substrate **2** was 83%. Based on the statistic goodness-of-fit (σ = 5.31, R^2 = 0.98), it can be concluded that the model describes the experimental data well.

Figure 7.

Since the enzyme is deactivated by substrates **1** and **2**, as well as by the intermediate **3**, it is very hard to obtain a high final concentration of **4** in a single batch reactor. Thus, the aldol reaction was further

performed in a repetitive batch [42] and fed-batch reactor configuration. By supplying the substrates into the reactor their concentration can be maintained at lower level, by which the enzyme operational stability decay can be lowered, or even minimized. The enzyme should also be added into the reactor to maintain its activity due to the inevitable operational stability decay. The repetitive technique has been shown to be very effective and easy to handle. [43] Additionally, this type of reactor could be a promising alternative to a batch reactor for producing higher concentrations of **4** by having not only additions of substrates, but also fresh enzyme. Therefore, the reaction was carried out in a repetitive batch reactor configuration with three additions of fresh substrates and enzyme without removal of the synthesized product (Figure 8), as **4** does not have a negative impact on the enzyme. According to our knowledge, this type of reactor has not yet been described for the DERA-catalyzed reaction of **2** with **1**. The usual reactor employed for the aldol reaction of **1** with **2** catalyzed by DERA, either as an isolated enzyme or as a whole-cell catalyst, were the batch reactor [4,5,12,16,19-21] and, to a lower extent, the fed-batch reactor [4,6,20].

The concentration of **1** was dosed in surplus reflecting on its erosive consumption in the side reaction. [3] At 2.1 and 4.2 hours after the start of the reaction the second and the third fresh feed of substrates and enzyme were added into the reactor (Figure 8). After 24 hours the conversion of **1** and **2** was complete. The yield of product **4** was 96% (50 g/L), the selectivity **4**/**5** was 7.2 and the selectivity **4**/**3** was 20.1. The final product composition (*w*/*w* %) of the reaction mixture contained 3.2% of **3**, 87% of **4** and 9.7% of **5**. Enzymatic activity (Figure 8 C) is shown as a relative value taking into account that after each addition into the reactor its value is regarded as its maximum, defined as 1. The absolute activity after the second and third enzyme addition was higher for 18 and 50%, respectively, compared to the initial activity. The enzyme operational stability decay (Figure 8 C) occurred in all three batches and was somewhat faster than in the batch shown in Figure 7. A plausible reason is that this experiment was initiated with lower

enzyme concentration (10 mg/mL batch vs. 5 mg/mL repetitive batch), which caused a longer exposure of the enzyme to the negative effect of aldehydes.

Figure 8.

Model validation was also done in the fed-batch reactor with constant substrate (q_1) and enzyme supply (q_2) (Figure 9). At the end of the experiment (25 h), the final concentration of **4** was 70 g/L. The final product composition (*w*/*w* %) of the reaction mixture was 6.42% of **3**, 77.12% of **4** and 16.46% of **5**. The statistical output (σ = 24.27, R^2 = 0.93) was weaker than in the previous two types of investigated reactors. This can be attributed to relatively high concentration of aldehydes in the reaction mixture for which the samples have to be diluted before analysis. Additionally, due to the high concentration of the added crude enzyme (total enzyme addition of 20 mg/mL), the solution became more viscous, causing a sampling error. Despite the aforementioned difficulties, Fig. 9 shows that the model described the experimental data well.

Figure 9.

The single quadrupole MS detector allowed direct peak identification of all compounds present in the reaction mixture, and therefore the identities of all reaction products (**3**, **4** and **5**) were confirmed.

3.6 Mathematical model simulations

Based on the experiments carried out, it can be concluded that the main drawback of DERA^{Tm}-catalyzed statin side-chain production is the enzyme operational stability decay caused by aldehydes present in the reaction mixture. Therefore, the choice of an effective process design is of crucial importance to minimize the enzyme decay, which should lead to significant process improvement. To accomplish this, it is necessary to find the most effective reactor configuration. In the case of a rapidly deactivating biocatalyst that is not being recycled, which is the case with the applied DERA enzyme, discontinuous

reactors, such as the batch or semi-batch reactor, represent an optimal solution. [44,45] These reactors are preferred for small-scale production of highly priced products since high conversion can be achieved per one batch. This feature is also very important because high yield leads to the reduced cost of product separation and purification. In the enzyme catalysed reaction these reactors are not preferable if the reaction is strongly inhibited by a product, since in that case achieving a desirable product concentration can be quite difficult. [44] When the reaction is substrate inhibited its impact on the reaction rate can be avoided by dosing the substrate into the reactor. In case of the DERA enzyme, the product and substrate inhibition did not occur, while the impact of the substrate on the DERA stability was significant. Because of it, the batch reactor with a defined substrate feeding is a promising strategy in order to minimize the enzyme operational stability decay.

Since the statistic output of the proposed model, together with the estimated kinetic parameters (Tables 2 and 3), was satisfactory for all types of investigated reactors, the model was used for the predictions of this reaction system in different reactor configurations. The model simulations were performed by changing the initial conditions in the batch and fed-batch reactor.

The concentration of **4**, its conversion yield (*Y*, calculated as the ratio of produced **4** and total amount of added **2**), productivity (*Pr*, g_4/(L day)) and biocatalyst yield (*BY*, g_4/g_{DERA}) were taken as the measure of process relevant outputs of the tested systems. [46] The bottleneck of this process is the enzyme stability, [15,20] and to optimize this process it is necessary to find the minimal enzyme concentration at which the optimal product yield and productivity will be accomplished. Thus, the simulations were performed by varying the enzyme concentration and its supply into the reactor. To minimize enzyme operational stability decay in the batch reactor caused by aldehyde substrates, fresh substrate additions were considered as well. Therefore, three different configurations of batch reactor were investigated: **BR1** – batch reactor in which the total amount of substrates and enzyme were added at the beginning of the

process, **BR2** – repetitive batch reactor in which the total amount of enzyme was added at the beginning of the process combined with three sequential substrate additions, and **BR3** – repetitive batch reactor with three sequential additions of substrates and enzyme. In the last two configurations (**BR2** and **BR3**) extra substrates and enzyme additions were simulated when yield **4** was 80%. The simulations were stopped when the final yield of **4** was 99% or at the time of 24 h. The results of those simulations are shown in Figure 10.

Figure 10.

The product **4** belongs to the category of pharmaceutical compounds. [4] According to the industrial requirements for this kind of compounds, the minimum biocatalyst yield must be 10 g/g, and the final product concentration must be at least 50 g/L to become economical. [4,21,46] Also, the total product yield should be at least 80%. Regarding the product concentration and yield, all three reactor types can satisfy this demand, however enzyme concentration is crucial. **BR1** required enzyme addition of at least 40 mg/mL, while in **BR2** and **BR3** the requirements were reached at enzyme concentrations of 15 mg/mL. The highest *BY* was achieved as in **BR2**, but at an enzyme concentration of 5 mg/mL at which the required concentration of **4** was not achieved. Taking into account the *Pr*, c_4 and *BY*, **BR2** ended being the optimal reactor configuration if the total enzyme addition of 15 mg/mL is applied. At that DERA^{Tm} concentration, the same *BY* was achieved in **BR3**, but with lower *Pr*. Nevertheless, in all tested batch reactor configurations, the industrial requirement for the *BY* were not accomplished.

For the fed-batch reactor simulation, different conditions of enzyme supply were examined; while the substrates were continuously fed into the reactor in all tested configurations. Three different ways of enzyme additions were investigated: **FBR1** – fed-batch reactor with enzyme addition only through feed, **FBR2** – fed-batch reactor with the addition of half of the amount of the enzyme at the start of the process and half of the amount through feed, and **FBR3** – fed-batch reactor with the addition of the total

amount of the enzyme at the beginning of the process. Simulations were stopped at time of 33.33 h (2000 min) and at that moment the *BY* and *Pr* were calculated (Figure 11).

Figure 11.

The yield of at least 80% was achieved at total enzyme additions of 0.4, 0.18, 0.16 g for **FBR1**, **FBR2** and **FBR3**, respectively. The highest *BY* was noted at 0.18 g of overall DERA^{Tm} addition for **FBR1** (6.57 g_4/g_{DERA}), 0.2 g for **FBR2** (10.16 g_4/g_{DERA}) and 0.18 g for **FBR3** (9.25 g_4/g_{DERA}). At those points, the final concentration of **4** was above 70 g/L. **FBR2** (total enzyme addition of 0.2 g) was chosen as the optimal reactor configuration for the fed-batch system based on the highest *BY*, since all other indicators (*Y*, c_4 and *Pr*) were similar under all conditions of enzyme supply studied.

Based on the simulations, it was concluded that the requirements for product concentration as well as for yield were achieved in both types of studied reactors. The batch reactor did not achieve the desired *BY* and therefore this type of reactor did not prove to be a good choice. The model was experimentally validated for the optimal reaction conditions in the fed-batch reactor since this type of reactor satisfied all requirements. The results are shown in Figure 12.

Figure 12.

The obtained experimental results are in good agreement with the mathematical model simulation. At 33 h the concentration of **4** was 78 g/L, *Pr* was 56 g_4/(L day) and *Y* was 95%. The final product composition (*w*/*w* %) of the reaction mixture was 10.35% of **3**, 2.28% of **4** and 87.37% of **5**. The statistical analysis provided by *Scientist* (σ = 6.95, R^2 = 0.99) proved that the experimental data are in good agreement with the predicted model simulations.

Even though DERA^{Tm} does not seem to be a very promising catalyst in the studied reaction regarding productivity, as it was 13-17 fold lower than the ones reported for other DERA enzymes (improved DERA

from *E coli* and DERA from *L. brevis*), [6,20,21] our study performed with this enzyme can be of general interest for this reaction in the future. Namely, while this reaction shows to have a strong potential for industrial application, one of the drawbacks is the lack of a detailed approach through the application of mathematical modelling techniques, as these enable process optimization important for process scale-up. It was shown and proven that in case of this specific reaction, the optimization of process parameters and process design can be done by the development and use of a mathematical model, which besides kinetic equations also includes mathematical description of enzyme operational stability decay dependencies on the compounds present in the reaction mixture.

4. Conclusion

For the studied reaction catalyzed by DERA^{Tm} a mathematical model was developed, which besides the kinetic and reactor model also includes the model for an enzyme operational stability decay. Kinetic parameters and operational stability decay rate were estimated by independent measurements. The developed model was successfully validated in the batch and fed-batch reactor and was used for the optimization of reaction conditions, in order to achieve optimal biocatalyst yield, product concentration and volume productivity. To minimize the enzyme operational stability decay, different conditions of enzyme and substrate supply were considered. Experimental results confirmed model simulations and a product concentration of 78 g/L, productivity of 56 g_4/(L day) and yield of 95% were achieved. According to our knowledge, this is the first time that mathematical model simulations were successfully applied for the optimization of the statin side-chain production catalyzed by the aldolase DERA. The used methodology should be an exceptional base for making this reaction industrially relevant.

Conflicts of interest

There are no conflicts to declare.

Acknowledgements

This work was supported by funding from the European Union's Horizon 2020 research and innovation program under Grant Agreement No. 635595 (CarbaZymes). The authors would like to thank Prozomix for the supply of DERA from *Thermotoga maritima* and Matija Cvetnić, MSc for the LC-MS analysis

References

1. Machajewski TD and Wong CH, The catalytic asymmetric aldol reaction. *Angew Chem Int Ed* **39**(8):1352-1374 (2000).

2. Dean SM, Greenberg WA and Wong CH, Recent advances in aldolase-catalyzed asymmetric synthesis. *Adv Synth Catal* **349**(8-9):1308-1320 (2007).

3. Ručigaj A and Krajnc M, Kinetic modeling of a crude DERA lysate-catalyzed process in synthesis of statin intermediates. *Chem Eng J* **259**:11-24 (2015).

4. Ručigaj A and Krajnc M, Optimization of a crude deoxyribose-5-phosphate aldolase lyzate-catalyzed process in synthesis of statin intermediates. *Org Process Res Dev* **17**(5):854-862 (2013).

5. Gijsen HJM and Wong CH, Sequential three- and four-substrate aldol reactions catalyzed by aldolases. *J Am Chem Soc* **117**(29):7585-7591 (1995).

6. Greenberg WA, Varvak A, Hanson SR, Wong K, Huang H, Chen P and Burk MJ, Development of an efficient, scalable, aldolase-catalyzed process for enantioselective synthesis of statin intermediates. *Proc Natl Acad Sci USA* **101**(16):5788–5793 (2004).

7. Fesko K and Gruber-Khadjawi M, Biocatalytic methods for C-C bond formation. *ChemCatChem* **5**(6):1248-1272 (2013).

8. Fessner WD, Aldolases: enzymes for making and breaking C-C bonds, in *Asymmetric organic synthesis with enzymes*, ed by Gotor V, Alfonso I and Garcia-Urdiales E. Wiley-VCH, Weinheim, pp. 275-319 (2008).

9. Sukumaran J and Hanefeld U, Enantioselective C–C bond synthesis catalysed by enzymes. *Chem Soc Rev* **34**(6):530-542 (2005).

10. Samland AK and Sprenger GA, Microbial aldolases as C–C bonding enzymes - unknown treasures and new developments. *Appl Microbiol Biotechnol* **71**(3):253-264 (2006).

11. Chen L, Dumas DP and Wong CH, Deoxyribose-5-phosphate aldolase as a catalyst in asymmetric aldol condensation, *J Am Chem Soc* **114**(2):741-748 (1992).

12. Woo MH, Kim MS, Chung N and Kim JS,Expression and characterization of a novel 2-deoxyribose-5-phosphate aldolase from haemophilus influenzae Rd KW20. *J Korean Soc Appl Biol Chem* **57**(5):655−660 (2014).

13. Časar Z, Historic overview and recent advances in the synthesis of super-statins. *Curr Org Chem* **14**(8):816-845 (2010).

14. Nara TY, Togashi H, Ono S, Egami M, Sekikawa C, Suzuki Y, Masuda I, Ogawa J, Horinouchi N, Shimizu S, Mizukamia F and Tsunoda T, Improvement of aldehyde tolerance and sequential aldol condensation activity of deoxyriboaldolase via immobilization on interparticle pore type mesoporous silica. *J Mol Catal B: Enzym* **68**(2):181–186 (2011).

15. Sakuraba H, Yoneda K, Yoshihara K, Satoh K, Kawakami R, Uto Y, Tsuge H, Takahashi K, Hori H and Ohshima T, Sequential aldol condensation catalyzed by hyperthermophilic 2-deoxy-D-ribose-5-phosphate aldolase. *Appl Environ Microbiol* **73**(22):7427–7434 (2007).

16. You ZY, Liu ZQ and Zheng YGS, Characterization and application of a newly synthesized 2-deoxyribose-5-phosphate aldolase. *J Ind Microbiol Biotechnol* **50**:29-39 (2013).

17. Barbas CF, Wang YF and Wong CH, Deoxyribose-5-phosphate aldolase as a synthetic catalyst. *J Am Chem Soc* **112**(5):2013-2014 (1990).

18. Liu J, Hsu CC and Wong CH, Sequential aldol condensation catalyzed by DERA mutant Ser238Asp and a formal total synthesis of atorvastatin. *Tetrahedron Lett* **45**(11):2439–2441 (2004).

19. Gijsen HJM and C. H. Wong CH, Unprecedented asymmetric aldol reactions with three aldehyde substrates catalyzed by 2-deoxyribose-5-phosphate aldolase. *J Am Chem Soc* **116**(18):8422-8423 (1994).

20. Ošlaj M, Cluzeau J, Orkić D, Kopitar G, Mrak P and Časar Z, A highly productive, whole-cell DERA chemoenzymatic process for production of key lactonized side-chain intermediates in statin synthesis. *PLoS ONE* **8**(5):e62250 (2013).

21. Jiao X-C, Pan J, Xu G-C, Kong X-D, Chen Q, Zhang Z-J and Xu J-H, Efficient synthesis of a statin precursor in high space-time yield by a new aldehyde-tolerant aldolase identified from *Lactobacillus brevis*. *Catal Sci Technol* **5**(8):4048-4054 (2015).

22. Wu Q and Tao J, Biocatalysis, in *Green Techniques for Organic Synthesis and Medicinal Chemistry*, ed by Zhang W and Cue B. John Wiley & Sons, Chichester, pp. 217-240 (2012).

23. Jennewein S, Schürmann M, Wolberg M, Hilker I, Luiten R, Wubbolts M and Mink D, Directed evolution of an industrial biocatalyst: 2-deoxy-D-ribose 5-phosphate aldolase. *Biotechnol J* **1**(5):537–548 (2006).

24. Nasmetova SM, Ruzieva DM, Rasulova GA, Sattarova RS and Gulyamova T, Effect of the principal nutrients on simvastatin production by wild strain Aspergillus terreus 20 in submerged fermentation. *Int J Curr Microbiol Appl Sci* **4**(9):894-898 (2015).

25. Schürmann M, Wolberg M, Panke S and Kierkels H, The development of short, efficient, economic, and sustainable chemoenzymatic processes for statin side chains, in *Green chemistry in the pharmaceutical industry*, ed by Dunn PJ, Wells AS and Williams MT. Wiley-VCH Verlag GmbH & Co. KGaA, Weinheim, pp. 127-144 (2010).

26. DeSantis G, Liu J, Clark DP, Heine A, Wilson IA and Wong CH, Structure-based mutagenesis approaches toward expanding the substrate specificity of D-2-deoxyribose-5-phosphate aldolase. *Bioorg Med Chem* **11**(1):43–52 (2003).

27. Subrizi F, Crucianell M, Grossi V, Passacantando M, Botta G, Antiochia R and Saladino R, Versatile and efficient immobilization of 2-deoxyribose-5-phosphate aldolase (DERA) on multiwalled carbon nanotubes. *ACS Catal* **4**(9):3059-3068 (2014).

28. Wang A, Wang M, Wang Q, Chen F, Zhang F, Li H, Zeng Z and Xie T, Stable and efficient immobilization technique of aldolase under consecutive microwave irradiation at low temperature. *Bioresour Technol* **102**(2):469–474 (2011).

29. Wang A, Gao W, ZhangF, Chen F, Du F and Yin X, Amino acid-mediated aldolase immobilisation for enhanced catalysis and thermostability. *Bioprocess Biosyst Eng* **35**(5):857-863 (2012).

30. Fei H, Zheng C, Liu X and Li Q, An industrially applied biocatalyst: 2-Deoxy-d-ribose-5-phosphate aldolase. *Process Biochem* **63**(1):55-59 (2017).

31. Lee L and Whitesides GM, Enzyme-catalyzed organic synthesis: a comparison of strategies for *in situ* regeneration of NAD from NADH. *J Am Chem Soc* **107**(24): 6999-7008 (1985).

32. Vasić-Rački Đ, Kragl U and Liese A, Benefits of enzyme kinetics modelling, *Chem Biochem Eng Q* **17**(1):7–18 (2003).

33. Pollard DJ and Woodey JM, Biocatalysis for pharmaceutical intermediates: the future is now. *Trends Biotechnol* **25**(2):66–73 (2007).

34. Sudar M, Findrik Z, Vasić-Rački Đ, Clapés P and Lozano C, Mathematical model for aldol addition catalyzed by two d-fructose-6-phosphate aldolases variants overexpressed in *E. coli*, *J Biotechnol* **167**(3):191–200 (2013).

35. Suau T, Álvaro G, Benaiges MD and López-Santín J, Kinetic modelling of aldolase-catalyzed addition between dihydroxyacetone phosphate and (*S*)-alaninal. *Biochem Eng J* **4**(1):95–103 (2008).

36. Garrabou X, Castillo JA, Guérard-Hélaine C, Parella T, Joglar J, Lemaire M and Clapés P, Asymmetric self- and cross-aldol reactions of glycolaldehyde catalyzed D-fructose-6-phosphate aldolase. *Angew Chem Int Ed,* **48**(30):5521-5525 (2009).

37. Beadford MM, A rapid and sensitive method for the quantitation of microgram quantities of protein utilizing the Principle of protein-dye binding. *Anal Chem* **72**(1-2):248-254 (1976).

38. SCIENTIST handbook. Micromath, Salt Lake City, pp. 110-300 (1986-1995).

39. Clapés P, Aldol reactions, in *Biocatalysis in organic synthesis*, vol. 2, ed by Faber K, Fessner W-D and Turner NJ. Georg Thieme Verlag KG, Stuttgart, pp. 31-92 (2015).

40. Presečki AV, Pintarić L, Švarc A and Vasić-Rački Đ,Different strategies for multi-enzyme cascade reaction for chiral vic-1,2-diol production, *Bioprocess Biosyst Eng*, **41**(6):793-802 (2018) .

41. Vasić-Rački Đ, Findrik Z and Presečki, AV, Modelling as a tool of enzyme reaction engineering for enzyme reactor development, *Appl Microbiol Biotechnol*, **91**(4):845–856 (2011).

42. Srinivasan B and Bonvin D, Controllability and stability of repetitive batch processes. *J Process Control* **17**(3):285–295 (2007).

43. Kragl U, Gödde A and Wandrey C, Repetitive batch as an efficient method for preparative scale enzymic synthesis of 5-azido-neuraminic acid and 15N-L-glutamic acid. *Tetrahedron: Asymmetry* **4**(6):1193-1202 (1993).

44. Bommarius AS, Riebel-Bommarius B. Biocatalysis, Wiley-Blackwell, Darmstadt, pp. 94-97 (2004).

45. Foutch GL, Johannes AH Reactors in Process Engineering in *Encyclopedia of Physical Science and Technology*, ed by Meyers RA, Elsevier Science Ltd, pp. 23-43 (2001).

46. Tufvesson P, Lima-Ramos J, Al Haque N, Gernaey KV and Woodley JM, "Advances in the process development of biocatalytic processes. *Org Process Res Dev* **17**(10):1233-1238(2013).

Table 1. Parameters of the polynomial model for the dependency of the operational stability decay constant on the concentration of **1**, **2** and **3**.

Aldehyde	***a*** [$mM^{-2}\ min^{-1}$]	***b*** [$mM^{-1}\ min^{-1}$]	**Equation**
1	$2.70 \cdot 10^{-7}$	$5.18 \cdot 10^{-5}$	$k_d = a \cdot c^2 + b \cdot c$ (1)
2	$7.40 \cdot 10^{-7}$	$9.85 \cdot 10^{-5}$	
3	$5.49 \cdot 10^{-6}$	$3.27 \cdot 10^{-5}$	

Table 2. Estimated kinetic parameters and the kinetic model for the double aldol addition of **1** and **2** and for the self-aldol addition of **1**.

Parameter	Unit	Value	Equation
First addition of 1 to 2			
V_{m1}	U mg^{-1}	1.92 ± 0.15	$r_1 = \frac{V_{m1} \cdot \gamma_{\mathbf{DERA}} \cdot c_1 \cdot c_2}{\left(K_{m1}^{\ 1} + c_1\right) \cdot \left(K_{m1}^{\ 2} + c_2\right)}$ (2)
$K_{m1}^{\ 1}$	mM	8.67 ± 1.85	
$K_{m1}^{\ 2}$	mM	37.63 ± 5.55	
Second addition of 1 to 3			
V_{m2}	U mg^{-1}	0.35 ± 0.04	$r_2 = \frac{V_{m2} \cdot \gamma_{\mathbf{DERA}} \cdot c_1 \cdot c_3}{\left(K_{m2}^{\ 1} + c_1\right) \cdot \left(K_{m2}^{\ 3} + c_3\right)}$ (3)
$K_{m2}^{\ 1}$	mM	1.43 ± 0.91	
$K_{m2}^{\ 3}$	mM	13.31 ± 2.18	
1 Self-aldol addition			
V_{m3}	U mg^{-1}	2.51 ± 0.21	$r_3 = \frac{V_{m3} \cdot \gamma_{\mathbf{DERA}} \cdot c_1^3}{\left(K_{m3}^{\ 1} + c_1\right)^2 \left(K_{m3}^{\ 1}\left(1 + \frac{c_2}{K_{i3}^{\ 2}}\right) + c_1\right)\left(1 + \frac{c_3}{K_{i3}^{\ 3}}\right)}$ (4)
$K_{m3}^{\ 1}$	mM	29.04 ± 3.01	
$K_{i3}^{\ 2}$	mM	0.14 ± 0.02	
$K_{i3}^{\ 3}$	mM	20.44 ± 250	

Table 3. Reactor models of the double aldol addition of **1** and **2** and the DERA^{Tm} operational stability decay constant model.

BATCH REACTOR	**FED-BATCH REACTOR**
$\frac{dc_1}{dt} = -r_1 - r_2 - r_3$ (5)	$\frac{dc_1}{dt} = \frac{c_{1,0} \cdot q_1 - c_1(q_1 + q_2)}{V} - r_1 - r_2 - r_3$ (11)
$\frac{dc_2}{dt} = -r_1$ (6)	$\frac{dc_2}{dt} = \frac{c_{2,0} \cdot q_1 - c_2(q_1 + q_2)}{V} - r_1$ (12)
$\frac{dc_3}{dt} = r_1 - r_2$ (7)	$\frac{dc_3}{dt} = -\frac{c_3(q_1 + q_2)}{V} + r_1 - r_2$ (13)
$\frac{dc_4}{dt} = r_2$ (8)	$\frac{dc_4}{dt} = -\frac{c_4(q_1 + q_2)}{V} + r_2$ (14)
$\frac{dc_5}{dt} = \frac{1}{3} r_3$ (9)	$\frac{dc_5}{dt} = -\frac{c_5(q_1 + q_2)}{V} + \frac{1}{3} r_3$ (15)
$\frac{d\gamma_{DERA}}{dt} = -k_d \cdot \gamma_{DERA}^2$ (10)	$\frac{d\gamma_{DERA}}{dt} = \frac{\gamma_{DERA,0} \cdot q_2 - \gamma_{DERA}(q_1 + q_2)}{V} - k_d \cdot \gamma_{DERA}^2$ (16)
	$\frac{dV}{dt} = q_1 + q_2$ (17)
OPERATIONAL STABILITY DECAY RATE CONSTANT MODEL	
$k_d = \sum_{i=1-3} (a_i \cdot c_i^2 + b_i \cdot c_i)$ (18)	

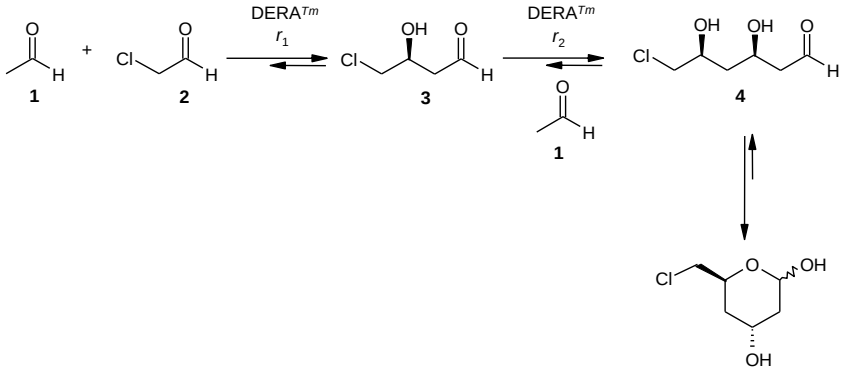

Figure 1. The reaction scheme of the DERA^{Tm} catalyzed aldol addition of acetaldehyde and chloroacetaldehyde.

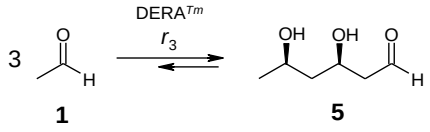

1 **5**

Figure 2. Self-aldol addition of **1** catalyzed by DERA^{Tm}.

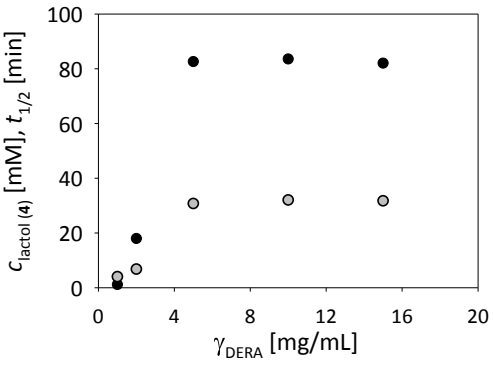

Figure 3. Enzyme half-life and resulting concentration of **4** at different enzyme concentrations in the batch reactor (c_1 = 200 mM, c_2 = 100 mM, 0.1 M TEA-HCl buffer, pH 7.0, 25 °C, γ_{DERA} = 1; 2; 5; 10; 15 mg/mL). Legend: black circles – **4**, grey circles – $\mathbf{t_{1/2}}$.

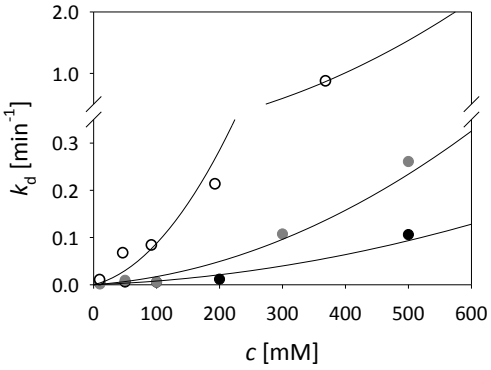

Figure 4. The influence of the concentration of **1**, **2** and **3** on the DERA^{Tm} operational stability decay constant (k_d) (0.1 M TEA-HCl buffer pH 7.0, 25 °C, γ_{DERA} = 10 mg /mL). Legend: black circles – **1**, grey circles – **2**, white circles – **3**, line – model.

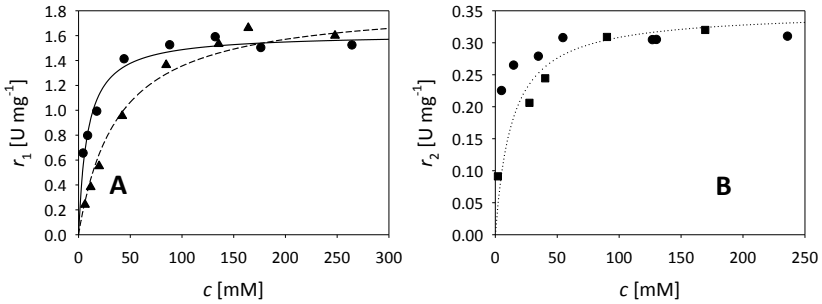

Figure 5. Kinetics of the tandem aldol addition of **1** and **2** catalyzed by DERA^{Tm} (0.1 M TEA-HCl buffer, pH 7.0, 25 °C, γ_{DERA} = 1 mg/mL). A) First aldol addition, the dependence of initial reaction rate on **1** ($c_{\mathbf{2}}$ = 200 mM) and **2** ($c_{\mathbf{1}}$ = 200 mM). B) Second aldol addition, the dependence of initial reaction rate on **1** (c_3 = 96.4 mM) and **3** (c_1 = 200 mM). Legend: experiment: circles – **1**, triangles – **2**, squares – **3**; model: line – **1**, dashed – **2**, dotted – **3**.

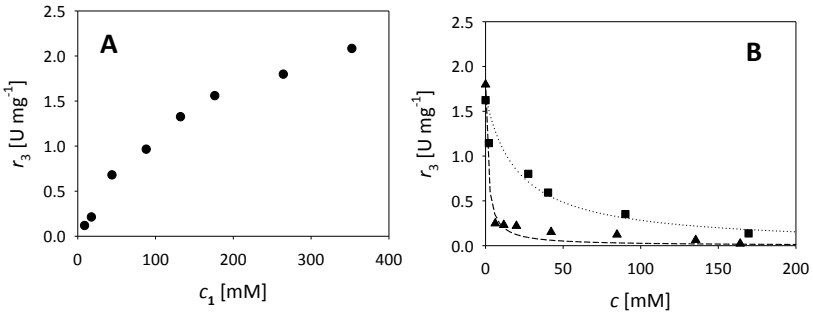

Figure 6. Kinetics of self-aldol addition catalyzed by DERA^{Tm} (0.1 M TEA-HCl buffer pH 7.0, 25 °C, γ_{DERA} = 1 mg/mL). A) The dependence of initial reaction rate on **1.** B) Impact of **2** and **3** on the initial reaction rate (c_1 = 200 mM). Legend: experiment: circles –**1**, triangles – **2**, squares – **3**; model: line – **1**, dashed – **2**, dotted – **3**).

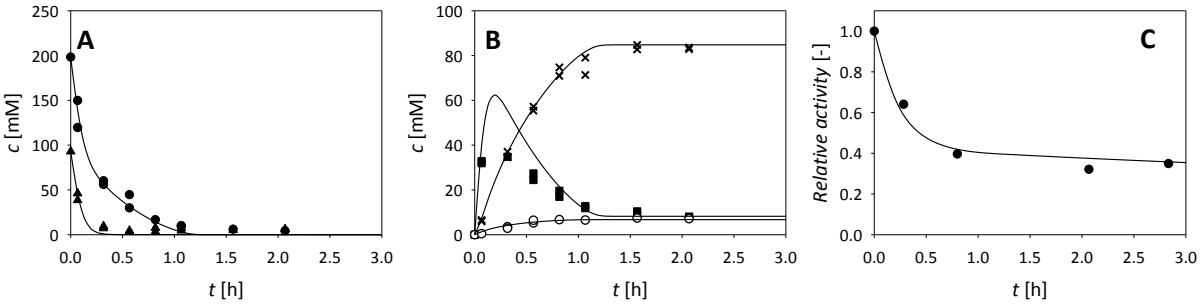

Figure 7. Double aldol addition of **1** to **2** in a batch reactor catalyzed by DERA^{Tm} (0. 1 M TEA-HCl buffer, pH 7.0, c_1 = 198 mM, c_2 = 93 mM, γ_{DERA} = 10 mg/mL). Time change of: A. substrate concentration (circles – **1**, triangles – **2**), B. product concentration (squares – **3**, x – **4**, empty circles – **5**) and C. enzyme activity (line – model).

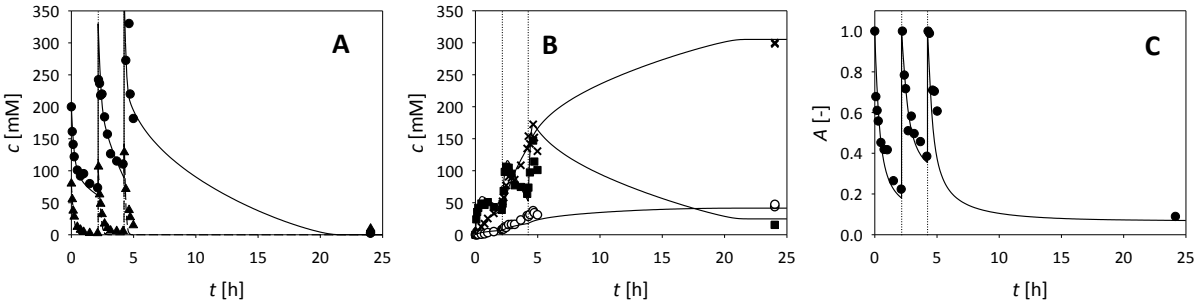

Figure 8. Double aldol addition of **1** to **2** in the repetitive batch reactor catalyzed by DERA^{Tm} (0.1 M TEA-HCl buffer, pH 7.0, c_1 = 200 (+257+270) mM, c_2 = 80 (+107+135) mM, γ_{DERA} = 5 (+5+5) mg /mL, 2nd addition – 2.1 h, 3rd addition – 4.1 h). Time change of: A. substrate concentration (circles – **1**, triangles – **2**), B. product concentration (squares – **3**, x – **4**, empty circles – **5**) and C. relative enzyme activity (line – model).

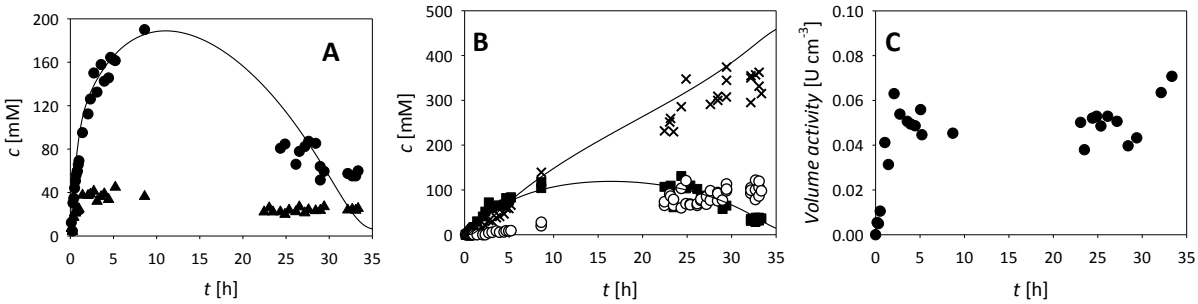

Figure 9. Double aldol addition of **1** to **2** in the fed-batch reactor catalyzed by DERA^{Tm} (0.1 M TEA-HCl buffer, pH 7.0, V_0 = 6 mL; feed 1: q_1 = 5 µL/min, $c_{\mathbf{1},0}$ = 2450 mM, $c_{\mathbf{2},0}$ = 950 mM; feed 2: q_2 = 2 µL/min, $\gamma_{DERA,F}$ = 100 mg/mL). Time change of: A. substrate concentration (circles – **1**, triangles – **2**), B. product concentration (squares – **3**, x – **4**, empty circles – **5**) and C. enzyme activity (line – model).

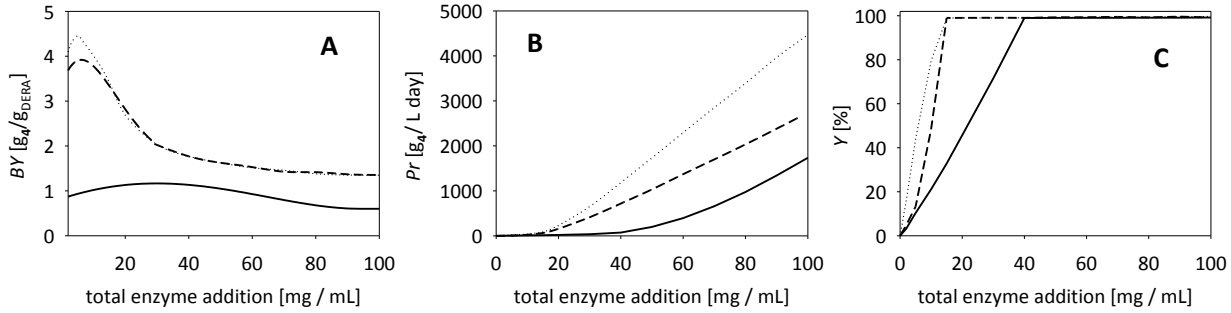

Figure 10. Simulations of double aldol addition of **1** to **2** catalyzed by DERA^{Tm} in different batch reactor configurations (**BR1**: c_1 = 741 mM, c_2 = 300 mM; **BR2** and **BR3**: c_1 = 230 x 3 mM, c_2 = 100 x 3 mM). Biocatalyst yield (A) productivity (B) and yield (C) change by total enzyme addition (line – **BR1**, dotted – **BR2**, dashed – **BR3**).

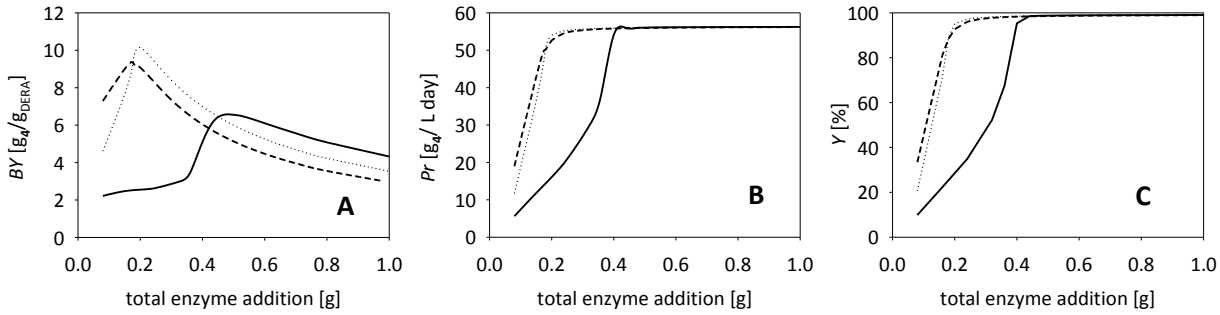

Figure 11. Simulations of double aldol addition of **1** to **2** catalyzed by DERA^{Tm} in different modes of fed-batch reactors (feed 1: q_1 = 5 µL/min; $c_{\mathbf{1},0}$ = 2300 mM, $c_{\mathbf{2},0}$ = 950 mM, **FBR1** and **FBR2**: V_0 = 6 mL; feed 2: q_2 = 2 µL/min; **FBR3**: V_0 = 10 mL). Biocatalyst yield (A) , productivity (B) and yield (C) change by total enzyme addition (line – **FBR1**, dotted – **FBR2**, dashed – **FBR3**).

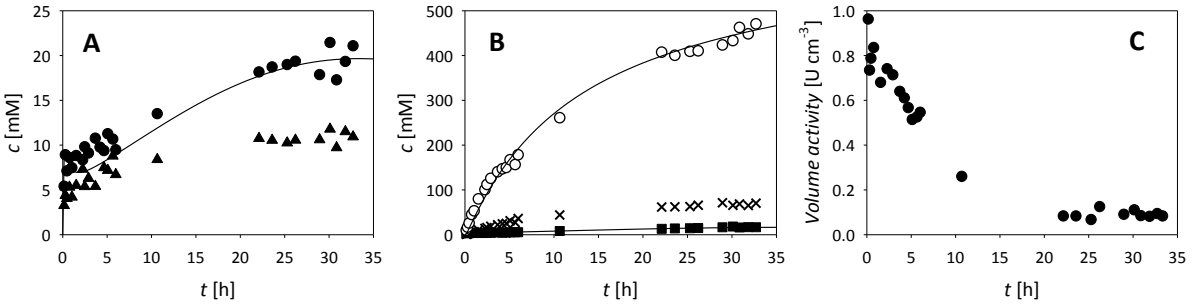

Figure 12. Testing the optimal conditions obtained by model based optimization in the reaction of double aldol addition of **1** to **2** in a fed-batch reactor catalyzed by DERA^{Tm} (0.1 M TEA-HCl buffer pH 7.0, V_0 = 6 mL, γ_{DERA} = 16.67 mg/mL; feed 1: q_1 = 5 µL min^{-1}, $c_{\mathbf{1},0}$ = 2300 mM, $c_{\mathbf{2},0}$ = 950 mM; feed 2: q_2 = 2 µL /min, $\gamma_{DERA,F}$ = 25 mg/mL). Time change of: A. substrate concentration (circles – **1**, triangles – **2**), B. product concentration (squares – **3**, x – **4**, empty circles – **5**) and C. enzyme activity (line-model).